Original Article

Institution of MECHANICAL ENGINEERS
Journal of MECHANICAL ENGINEERING SCIENCE

Proc IMechE Part C:
J Mechanical Engineering Science
2019, Vol. 233(7) 2563–2573

DOI: 10.1177/0954406218786976
journals.sagepub.com/home/pic
SAGE

Generalized optimization procedure for rotational magnetized direction permanent magnet thrust bearing configuration

Siddappa Iranna Bekinal[1], Mrityunjay Doddamani[2], Mohan Vanarotti[1] and Soumendu Jana[3]

Abstract

Optimization of rotational magnetized direction permanent magnet thrust bearing configuration is carried out using generalized three-dimensional mathematical model. The bearing features namely axial force and stiffness are maximized using in-house developed mathematical expressions solved using MATLAB. The design variables selected for the optimization are axial offset, number of ring pairs, air gap and inner radius of inner and outer rings. The maximized axial force values of the optimized configuration are validated with the finite element analysis results. To overcome the high computational cost associated with three-dimensional equations, generalized method of optimization is sucessfully demonstrated using plots representing variation of optimal design variables as a function of air gap with respect to bearing's outer diameter. Simple and useful method of using the generalized plots for the process of optimization is presented by dimension optimization of representative bearing configuration with a particular aspect ratio. The proposed optimization using mathematical model and generalized approach assists designer in selecting optimized geometrical parameters of rotational magnetized direction thrust bearing configurations easily for variety of high-speed applications.

Keywords

Permanent magnet thrust bearing, optimization, control volume, axial stiffness, axial force

Date received: 1 November 2017; accepted: 11 June 2018

Introduction

Increase in the utilization of permanent magnet (PM) bearings for both low[1–4] and high-speed[5–8] applications drives the researchers for detailed and critical analysis in design and optimization of bearing characteristics alongside the ease of manufacturing them. Many authors contributed towards the design in terms of two-dimensional (2D) analytical equations for bearing features using dipole[9–12] and Amperian methods.[13] Neverthless, curvature effect of rings is not addressed in their investigations. This necessitates the development of semi-analytical[14–18] models by incorporating the curvature effect. Lijesh and Hirani[19] modified 2D equations by considering the influence of the geometrical parameters on force and stiffness using statistical analysis and presented the optimization for radial load in a single-layer axially polarized radial permanent magnet bearing (PMB). Optimization of axially magnetized stack structured radial passive magnetic bearing is carried out by the Moser et al.[20] for maximum stiffness in a given control volume using 2D finite element analysis (FEA). The PM thrust bearings made of axially polarized multi-rings are optimized for maxiumum stiffness as well as axial force in Bekinal et al.[21] for a given control volume using 3D equations. Xu et al.,[22] Marth et al.,[23] Yoo et al.,[24] Safaeian and Heydari,[25] and Bekinal et al.[26] used 2D equations to optimize the conventional as well as Halbach PMB configurations. In the recent past, optimization is carried out by Beneden et al.[27] for all topologies of the PM thrust

[1]Sanjeevan Engineering and Technology Institute, Sanjeevan Knowledge City, Kolhapur, India
[2]Department of Mechanical Engineering, National Institute of Technology Karnataka, Surathkal, India
[3]Bearings and Rotor Dynamics Laboratory, Propulsion Division, National Aerospace Laboratories, Bengaluru, India

Corresponding author:
Siddappa Iranna Bekinal, Sanjeevan Engineering and Technology Institute, Sanjeevan Knowledge City, Somwar Peth-Injole, Panhala, Kolhapur 416201, Maharashtra, India.
Email: siddappa.bekinal@seti.edu.in

bearing using 2D analytical equations for the maximum force. Outcome of observations from the existing literature on optimization of PMB are: (i) 2D FEA and 2D analytical expressions lack precision compared to 3D equations in cases where mean radius is not large enough as compared to the air gap and the PM thickness are used, and (ii) assumption of equal radial thickness $((R_2-R_1)=(R_4-R_3))$ of inner and outer rings in the PM bearings resulting in partial optimization. Complete optimization of the rotational magnetized direction (RMD) configuration PM thrust bearings in a given control volume is yet to be addressed. Pragmatic optimization of axially stacked radial PMBs for the maximum radial load using 3D equations is presented in our earlier work.[28] The optimization of different PMB configurations: monolithic, conventional, and RMD is carried out based on the constraints, constants, and bounds of the dimensions obtained from published literature. The optimization of RMD configuration PM thrust bearing in a given control volume has not been addressed yet using 3D equations and there is need for generalizing the optimization procedure. These facts demand for the use of 3D equations for complete optimization of RMD configuration PM thrust bearings and generalizing the same in a given control volume and is dealt in the present work.

Three-dimensional equation for an axial force in PM bearings made up of n number of ring pairs[18] is generalized and adopted for the optimization process. The generalized equation is solved in MATLAB to conduct optimization for selected design variables in a given control volume. Axial force values of the optimized configuration calculated using proposed 3D equations are validated with FEA results. Optimized results are utilized to present the plots establishing the relationship between optimal design variables and air gap with respect to bearing outer diameter. Further, the usage of generalized plots for optimization of the PM thrust bearing is demonstrated using a suitable representative example. Finally, optimization results of conventional and RMD configuraions are compared and conclusions are summarized.

PM thrust bearing configurations

RMD thrust bearing configurations made up of two and multiple ring pairs are presented in Figure 1(a) and (b), respectively. The geometrical dimensions of both the configurations for which the same cylindrical volume is assumed is depicted in Figure 1. For maximization of the axial force and stiffness, chosen design variables are, axial offset (z), number of ring pairs (n), inner radius of inner rings (R_1), inner radius of outer rings (R_3), and air gap (g). The values of these variables are optimized for maximum values of bearing features using 3D mathematical model. An aspect ratio ($L/2R_4$) of 0.5 is selected for both the configurations under investigation. Geometrical dimensions selected for both the configurations in optimization are listed in Table 1.

Mathematical model

Three-dimensional equations for force and stiffness in axially, radially, and RMD stack structured PM bearings with n number of ring pairs are presented in Bekinal and Jana.[18] In RMD configuration, the total axial force exerted by the outer rings on inner one is due to the interaction between (i) axial–axial, (ii) radial–radial, and (iii) axial–radial or radial–axial polarized rings. The generalized equation for an axial force is presented in this article. The interaction between only axial–radial polarized rings is shown in Figure 2, whereas interaction between axial–axial and radial–radial polarized rings are presented in Bekinal et al.[5] Figure 2 shows the PM bearing with uth rotor and vth stator ring. The rotor on which uth

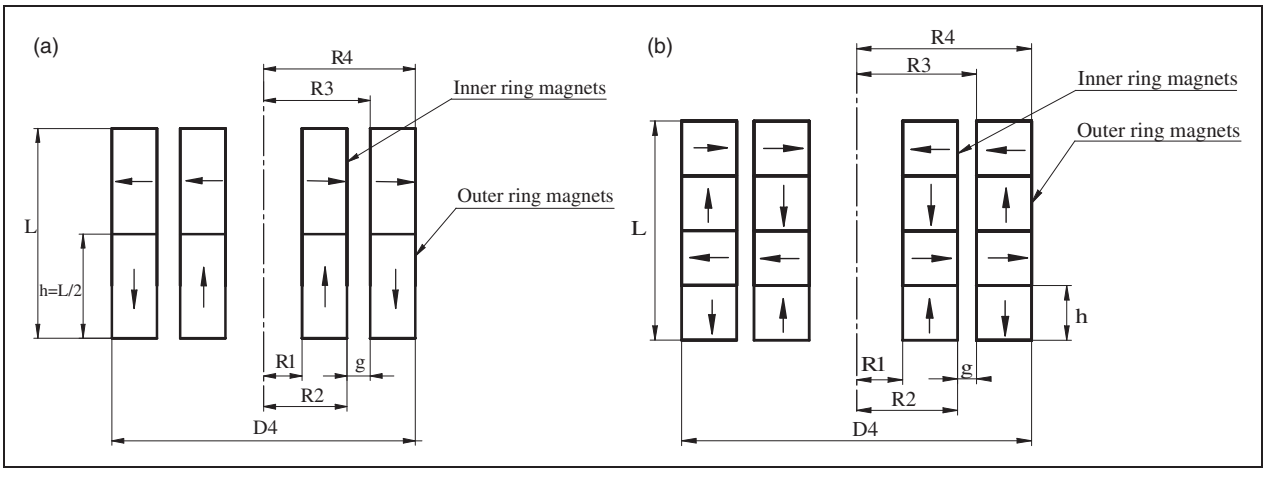

Figure 1. Constant control volume RMD thrust bearing configurations with: (a) two and (b) multiple ring pairs (stack structured configuration).

ring is mounted is free to move in Cartesian coordinate system with respect to vth stator ring. The length of both inner and outer rings is h in the axial direction. The fictitious charged surfaces of rotor and stator magnets are 1, 2, 3, and 4, respectively.

The resultant axial force generated on the inner rings in RMD thrust bearing configuration made up of n number of ring pairs arranged in XYZ coordinate system is expressed as

$$F_Z = \frac{B_r^2}{4\pi\mu_0}\sum_{u=1}^{n}\sum_{v=1}^{n}\sum_{k=1}^{2}\sum_{l=3}^{4}\sum_{p=1}^{m}\sum_{q=1}^{m}\frac{S_{pku}\,S_{qlv}}{R^3_{(pku)(qlv)}} \times \left(Z_{qlv} - Z_{pku}\right)(-1)^{(k+l)}(-1)^{(a)} \quad (1)$$

where m is the number of discrete elements on stator and rotor, S_{pku} is the surface area of pth element located on kth surface of uth rotor ring, S_{qlv} is the surface area of qth element located on lth surface of vth stator ring. The positions of the elements on the faces of rotor and stator are expressed as follows.

For odd values of u and v

$$\begin{aligned} X_{pku} &= (x + r_{mr}\cos\beta)\,\mathbf{i} & X_{qlv} &= (r_{ms}\cos\alpha)\,\mathbf{i} \\ Y_{pku} &= (y + r_{mr}\sin\beta)\,\mathbf{j} & Y_{qlv} &= (r_{ms}\sin\alpha)\,\mathbf{j} \\ Z_{pku} &= (z + (u-1)\,l)\,\mathbf{k} & Z_{qlv} &= (v\,l)\,\mathbf{k} \end{aligned} \quad (2)$$

For even values of u and v

$$\begin{aligned} X_{pku} &= (x + R2\cos\beta)\,\mathbf{i} & X_{qlv} &= (R4\cos\alpha)\,\mathbf{i} \\ Y_{pku} &= (y + R2\sin\beta)\mathbf{j} & Y_{qlv} &= (R4\sin\alpha)\,\mathbf{j} \\ Z_{pku} &= (z + l_m)\,\mathbf{k} & Z_{qlv} &= (l_m)\,\mathbf{k} \\ l_m &= l(g-1) + (j-1)\tfrac{l}{N_1} + \tfrac{l}{2N_1} \end{aligned} \quad (3)$$

where $g = u$ or v, and $u = 1, 2, 3,\ldots,n$, $v = 1, 2, 3,\ldots n$, N_1 is the number of element divisions on the polarized surfaces of rings and $j = 1, 2, 3,\ldots,N_1$.

The expression for a in equation (1) is calculated based on the following combination:

If u is even and odd and $(u+v)$ is even

$$a = \left(\frac{(u+v)}{2} - u\right) \quad (4)$$

If u is even and $(u+v)$ is odd

$$a = \left(\frac{(u+v+1)}{2} - u\right) \quad (5)$$

If u is odd and $(u+v)$ is odd

$$a = \left(\frac{(u+v-1)}{2} - u\right) \quad (6)$$

Table 1. Geometrical dimensions of the PM thrust bearing.

Paramater	Value
Inner radius of inner rings, R_1 (m)	0.009
Inner radius of inner rings, R_2 (m)	0.014
Inner radius of outer rings, R_3 (m)	0.015
Outer radius of bearing, R_4 (m)	0.02
Air gap, g (m)	0.001
Axial length, L (m)	0.02
Magnetic polarization, B_r (T)	1.2
Aspect ratio, $AR = L/2R_4$	0.5

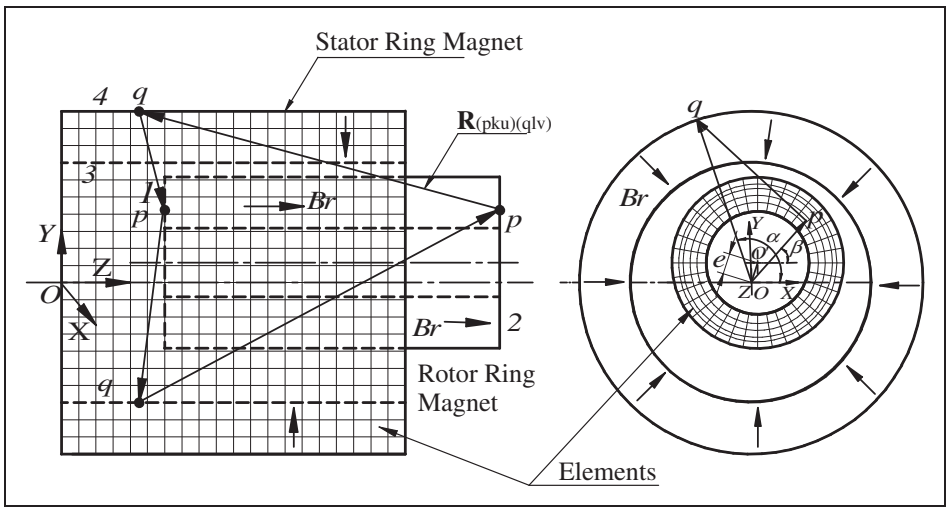

Figure 2. PM thrust bearing with stator and rotor rings: o – stator ring magnet center, o' – rotor ring magnet center, e – eccentricity of rotor center from stator center in meter, α – inclination of line joining the element on the stator surface and center o with the horizontal, and β – inclination of line joining the element on the rotor surface and center o with the horizontal.

The axial stiffness of the stack structured PMB is given by

$$K_z = -\frac{dF_Z}{dZ} = -\frac{1}{2\,\Delta Z}[F_Z(Z+\Delta Z) - F_Z(Z-\Delta Z)] \tag{7}$$

Equations (1) and (7) are solved in MATLAB to carry out the optimization.

Optimization

To maximize the characteristics of the PM thrust bearings, optimization of several relevant design variables such as axial offset, number of ring pairs, inner and outer radii of inner and outer rings, air gap and axial length of each ring pair selected for the given cylindrical volume is necessary. Optimization is carried out by considering two different cases of single-objective functions: (i) maximizing force and (ii) maximizing stiffness in a given control volume. The objective functions, constraints, constants, and bounds are written in the following format.

Objective function: Maximize either an axial force or axial stiffness i.e. $(F_z)_{\max}$ or $(K_z)_{\max}$

Constraint:

$$n \cdot h = L$$

where n is the number of ring pairs, h is the axial length of each ring pair, and axial length of a bearing (L) can be fixed by choosing the aspect ratio and outer diameter (D_4).

Constants: B_r=1.2 T

$D_4 = 40\,\text{mm},\ L = 20\,\text{mm}$ are fixed for an aspect ratio(L/D_4) of 0.5

Bounds: $[D_1,\ D_2,\ D_3,\ z]$

$0 \leqslant D_1 \leqslant 24\,\text{mm}$

$4 \leqslant D_3 \leqslant 38\,\text{mm}$

$D_2 = D_3 - 2g$

$0.25 \leqslant g \leqslant 2\text{mm}$ in steps of 0.25

$-(h+2) \leqslant z \leqslant 0\,\text{mm}$

The steps followed in the optimization process are as given below.

STEP 1: Variables R_4 and L are fixed to define constant cylindrical volume.

STEP 2: Variables axial offset (z), number of ring pairs (n), and air gap (g) are considered to be the most imporatant one among others due to their greater effect on bearing characteristics.[21] To understand the effetct of an axial offset, the axial force and stiffness are calculated for the selected configuration (Table 1) using developed 3D equations by increasing the number of ring pairs. Maximum force is generated at an axial offset of $z = -h$ (approximately) and h value depends upon the number of rings in the control volume. The axial stiffness is maximum at zero axial offset for all number of ring pairs. The axial offset value at which stiffness is maximum is independent of number of ring pairs.

STEP 3: For each air gap (0.25 to 2 mm insteps of 0.25 mm), the optimized value of the number of ring pairs (n_{opt}) is determined by varying the rings on the rotor and stator in the control volume.

STEP 4: Optimized values of R_1 are determined by fixing R_3 and n_{opt} for all values of air gaps.

STEP 5: R_3 is optimized by knowing the optimized values of z, n, and R_1 for different air gaps.

For the selected configuration, estimated axial force and stiffness values for different air gaps are presented in Figure 3 and are listed in Table 2. The optimization results show that the optimum

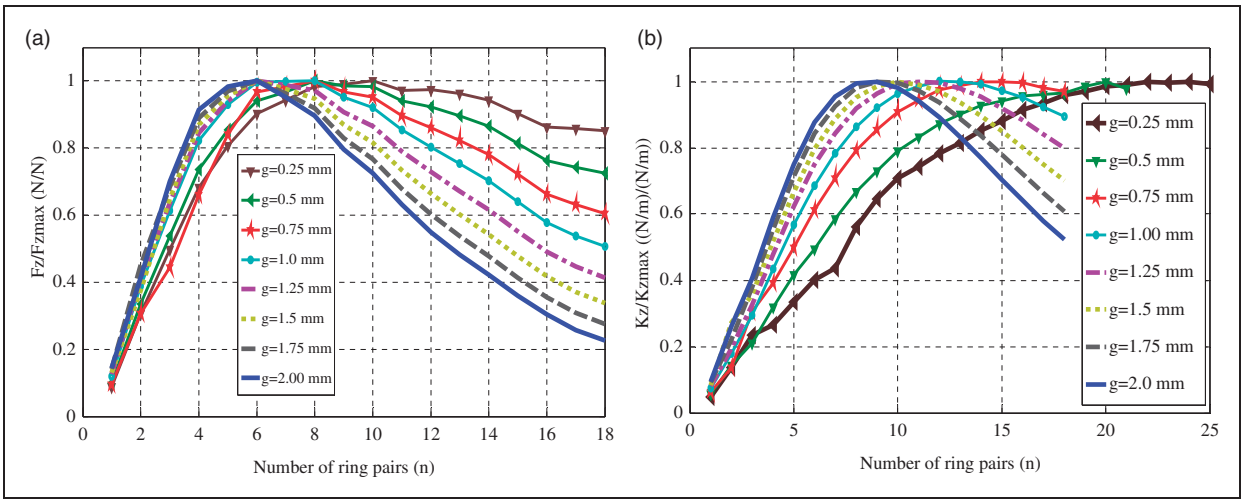

Figure 3. Optimum number of ring pairs for different air gaps at maximized values of: (a) axial force and (b) stiffness.

values of the number for ring pairs increase with the decrease in the air gap.

Based on the optimized values of axial offset (z_{opt}) and the number of ring pairs (n_{opt}) in the previous step, variables R_1 and R_3 are optimized. Optimized values of R_1 are plotted in Figure 4 with respect to air gap for maximum axial force and stiffness. Both maximal force and stiffness values increase with R_1 (shaft radius) up to a certain value and reaches their peak followed by abrupt decrease with further increase in the shaft radius. Lower influence of air gap on R_1 is noticed for both maximum stiffness and force. Results of Figure 4 depict approximate values of R_1 at which maximum force and stiffness are 0.006 and 0.009 m, respectively. Procedure adopted for the optimization of R_3 is similar to that of R_1. The axial force and stiffness values are graphed in Figure 5 with respect to R_3 for different air gap values. Results reveal that the optimized values of R_3 are 0.016 and 0.0165 m respectively with negligible effect of air gap.

Optimized values of design variables calculated for 1 mm air gap in the selected configuration are listed in

Table 2. Optimum number of ring pairs for different air gaps.

Air gap g (mm)	$(n)_{opt}$ for max. axial force	$(n)_{opt}$ for max. axial stiffness
0.25	10	24
0.5	8	20
0.75	8	14
1	8	12
1.25	6	11
1.5	6	10
1.75	6	9
2	6	9

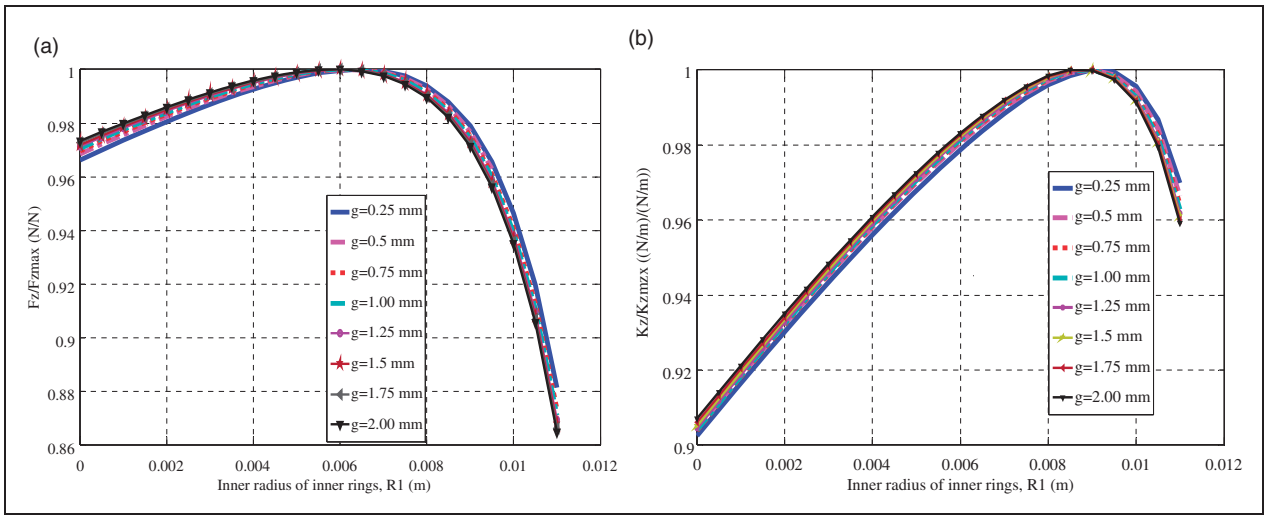

Figure 4. Optimum values of R_1 for different air gaps for maximized: (a) axial force and (b) stiffness values.

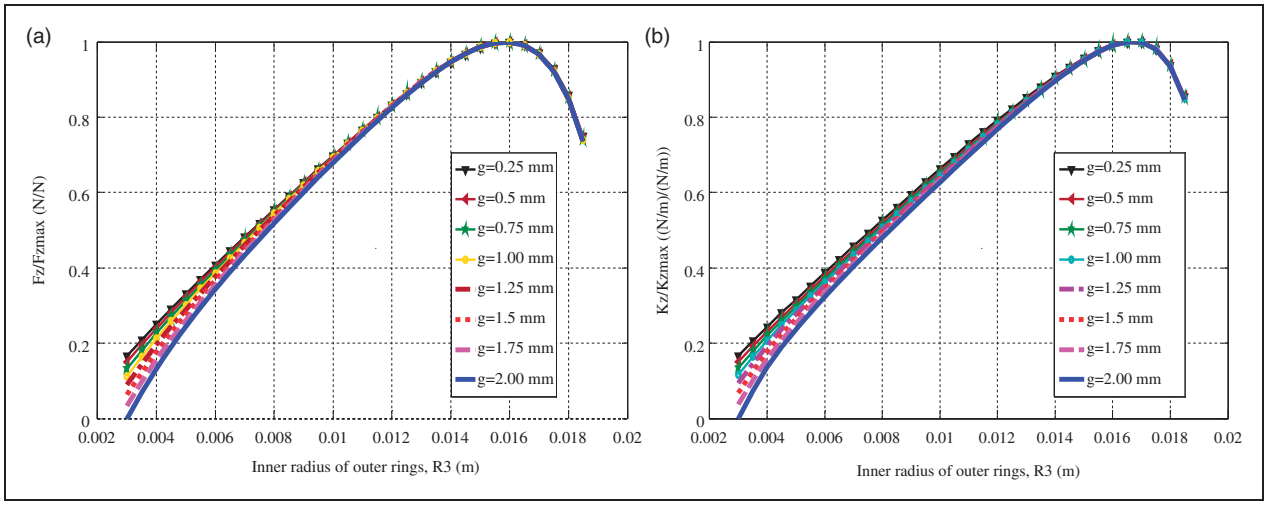

Figure 5. Optimum values of R_3 for different air gaps for maximized: (a) axial force and (b) stiffness values.

Table 3. Maximized force and stiffness values of optimized bearing along with values of two ring pairs for aspect ratio of 0.5 at 1 mm air gap are shown in Figure 6. The calculated maximum values of axial force and stiffness in the optimized configuration are 2.75 (771.49 N) and 6.29 times (588,737.2 N/m) respectively as compared to the two ring pairs on the bearing in a given control volume.

Validation of maximized values of an axial force

The selected RMD thrust bearing configuration with optimized geometrical dimensions (Table 3) is modeled and analyzed using 3D FEA in ANSYS V13. Neodymium iron boron (NdFeB) magnet rings (N35 grade) are selected on stator and rotor with magnetic properties as $B_r = 1.2\,\text{T}$, $H_c = 868\,\text{kA/m}$, and μ_r ($B_r/\mu_0 H_c$) = 1.1. The ring pairs in bearing configuration are modeled using 471,252 solid97 elements having 142,463 nodes by polarizing them in axial and radial directions (Figure 7(a)). The axial force (Figure 7(b)) acting on inner by outer rings is determined using magnetic virtual displacement method. Results of FEA along with mathematical model values for the optimized configurations are presented in Figure 7(c). Good agreement (10.75%) between optimization and FEA results is observed as depicted in Figure 7(c).

Table 3. Optimum values of design variables in RMD configuration PM thrust bearing.

Parameters	Optimized values for maximum axial force	Optimized values for maximum axial stiffness
z (m)	0.0025	0
n	8	12
R_1 (m)	0.006	0.009
R_2 (m)	0.015	0.0155
R_3 (m)	0.016	0.0165
R_4 (m)	0.02	0.02

Generalization of optimization procedure

Optimization of RMD thrust bearing configuration is carried out for an aspect ratio of 0.5. In this section, an attempt has been made to obtain generalized plots representing optimized values in terms of bearings' outer diameter with respect to an air gap. The obtained generalized plots can be used for selecting the optimized parameters of the PM thrust bearing of any aspect ratio. In addition, it is shown that the ends of the permanent magnet cylinders make constant contribution to the maximal axial force and stiffness values irrespective of the aspect ratios of the bearing in Moser et al.[20] and Bekinal et al.[21]

This section describes the procedure to assist designers for sizing rings of PM thrust bearing. Sizing is done in a control volume for PMB with a maximal axial force (zero stiffness) or a maximal axial stiffness (zero force). The designer has to select the parameters: external diameter of outer rings (D_4), the air gap (g), and the aspect ratio (AR) to compute the optimum number of rings (n_{opt}), optimum values of D_1 and D_3. Value of D_2 is to be estimated based on the values of air gap and D_3. This method is useful for all the values of aspect ratio and D_4 for an air gap range of 0.25–2 mm.

The relationship between the optimized parameters and the ratio of air gap to outer diameter (g/D_4) is used to present the generalized optimization

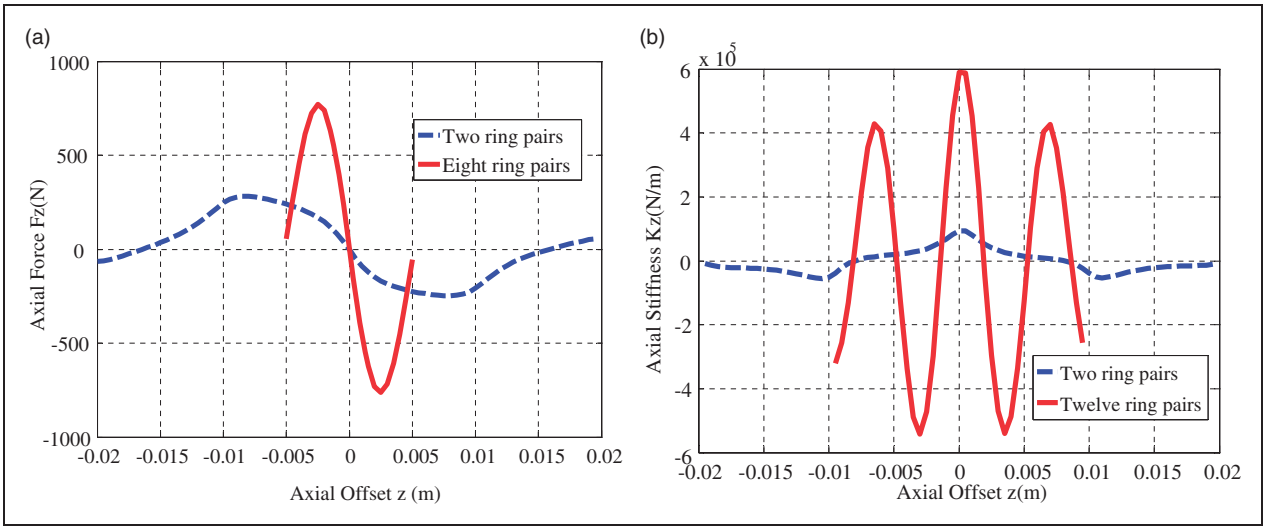

Figure 6. Maximized values of optimized bearing configuration along with results of configuration with two ring pairs: (a) axial force and (b) stiffness.

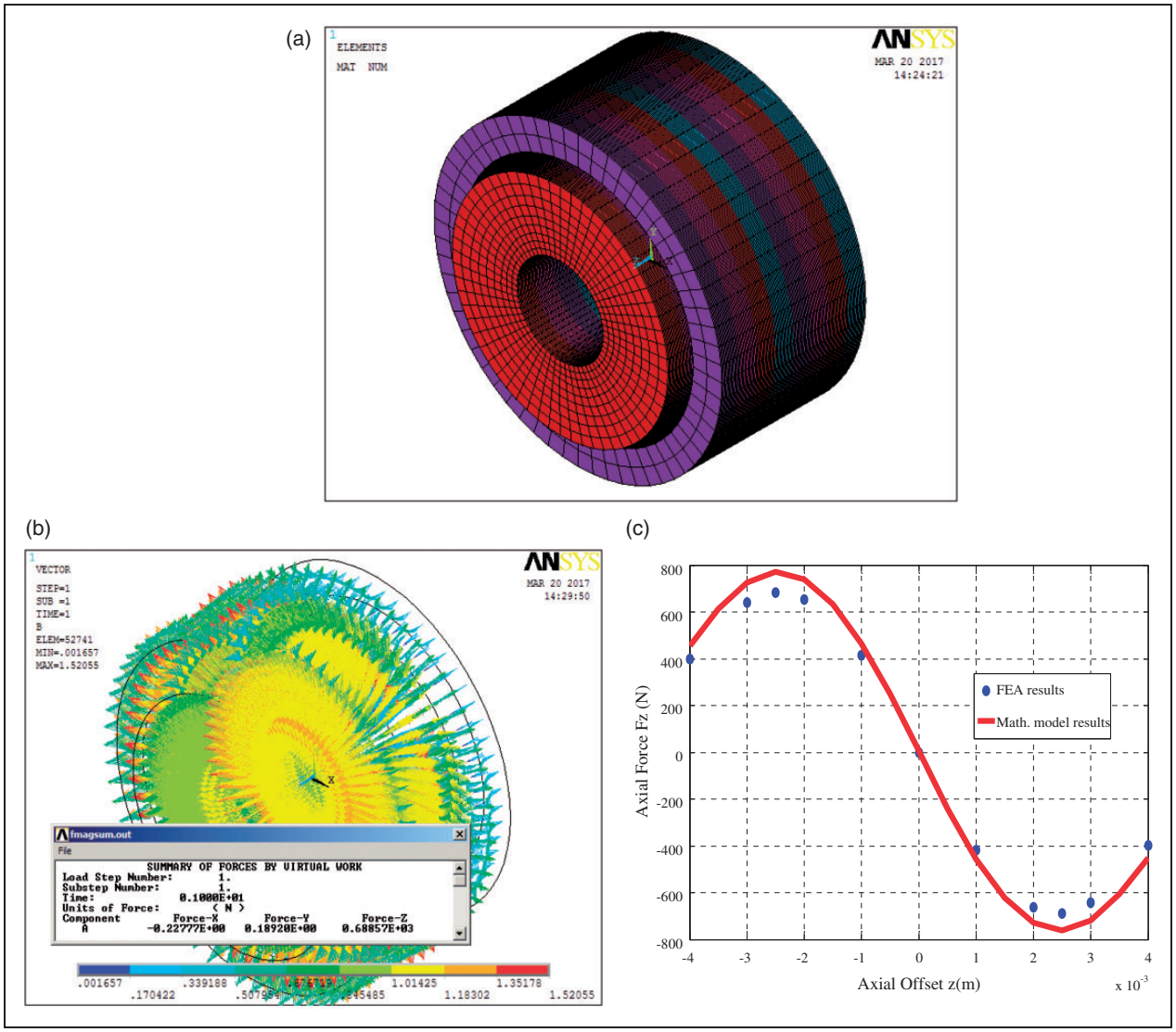

Figure 7. FEA results for: (a) elements on rotor and stator rings model, (b) maximum force generated in the optimized configuration, and (c) comparative plot.
FEA: finite element analysis.

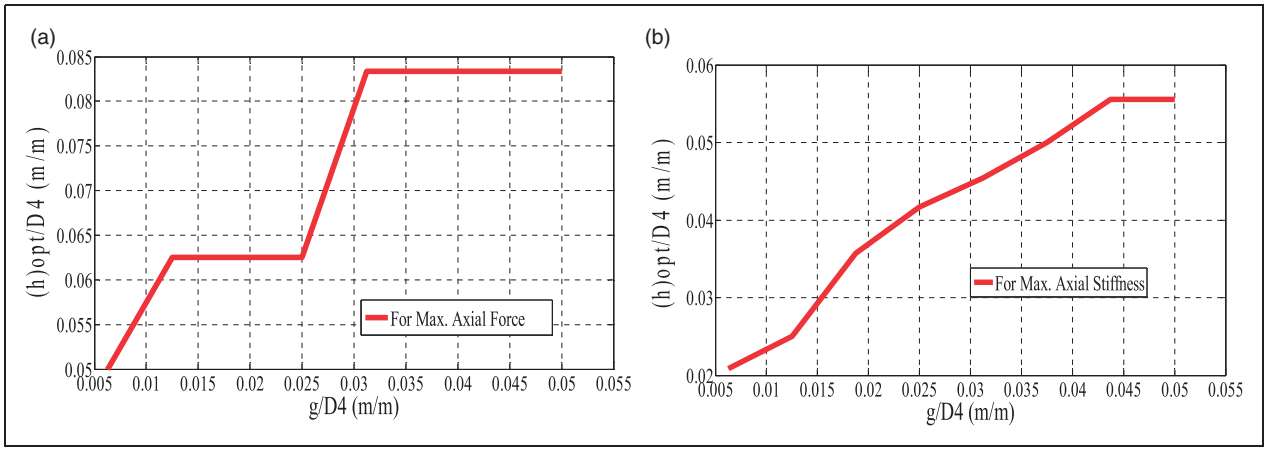

Figure 8. Optimum axial length of each magnet ring vs. air gap for the maximized values of: (a) axial force and (b) stiffness.

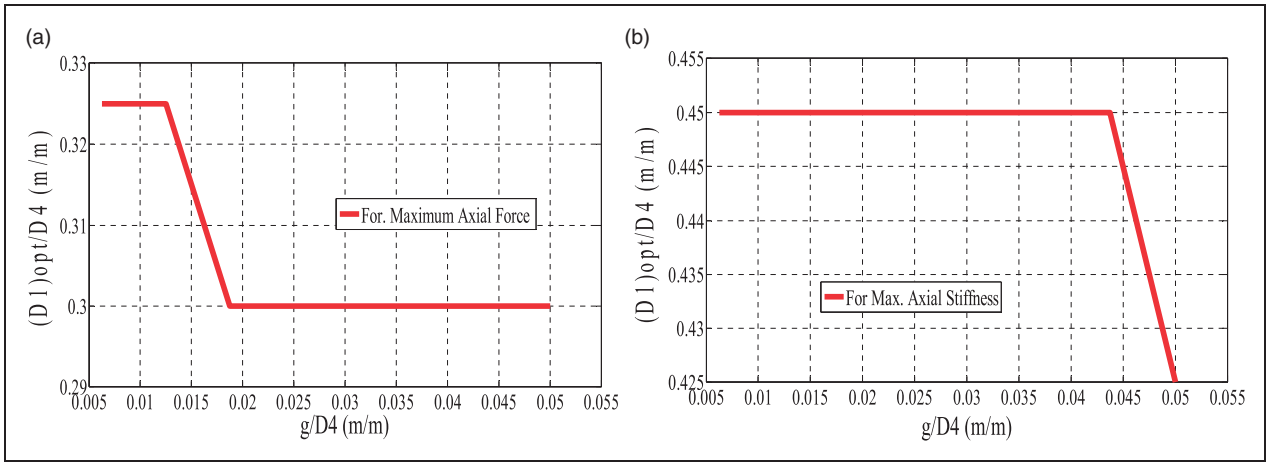

Figure 9. Optimized inner diameter of inner ring values as a function of air gap for the maximized values of: (a) axial force and (b) stiffness.

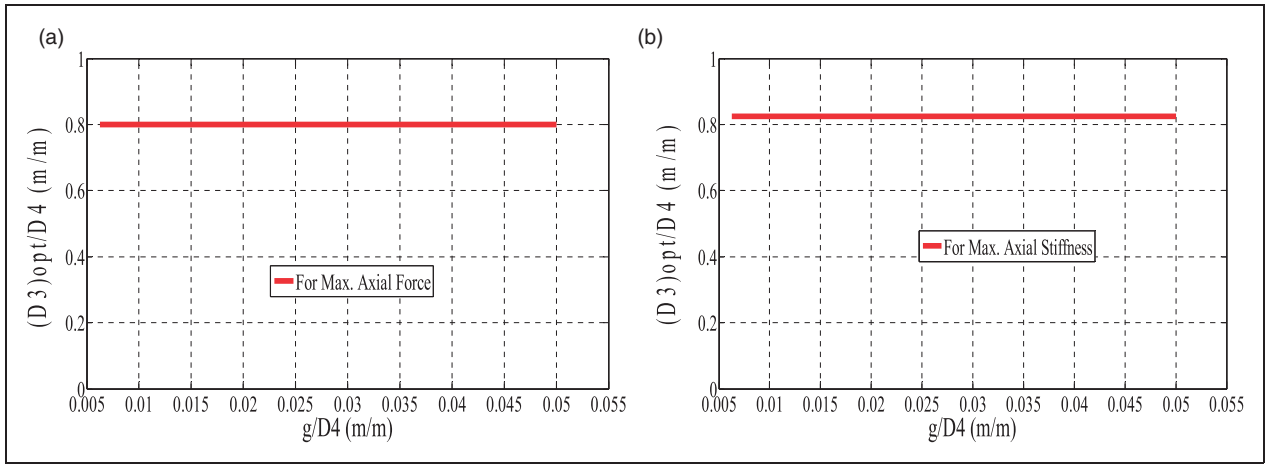

Figure 10. Optimized inner diameter of outer ring values vs. air gap for the maximized values of: (a) axial force and (b) stiffness.

procedure for PM thrust bearings. The generalized procedure can be used directly in the industry by the designers to select the optimum dimensions of multi-rings thrust bearing for generating the optimum bearing features. The plots representing $((h)_{opt} = L/n)/D_4$ vs. g/D_4, $((D_1)_{opt}/D_4)$ vs. g/D_4 and $(D_3)_{opt}/D_4$ vs. g/D_4 are presented in Figures 8 to 10. In addition, the optimum values of D_3/D_4 for different values of g/D_4 for optimum features are shown in Figure 11.

Based on the results of the relationship between the generalized variables, the following observations are noted for air gap ranging from 0.25 to 2 mm.

- For maximum force and stiffness, increase in the air gap increases the optimum value of the ring axial thickness (Figure 8).
- The optimum value of the inner diameter of rotor rings ($(D_1)_{opt}$) is constant for a certain value of air gap and then decreases abruptly with the increase in the air gap for both force and stiffness maximizations (Figure 9). Optimum value of shaft diameter decreases with the increase in the air gap.
- The optimum value of the inner diameter of stator rings is almost constant in both force and stiffness maximizations, which indicates that the influence of air gap on the optimum value of the inner diameter of stator rings is zero (Figure 10).

The procedure of referring to the generalized plots (Figures 8–10) for determining the optimum design variables in the PM thrust bearing is given below for designers reference. For RMD configuration, the PM thrust bearing has an aspect ratio of 0.75 i.e. $L = 0.0375$ m, $g = 1$ mm, and $D_4 = 0.05$ m, and the steps to be followed to calculate the optimized values of dimensions are:

1. The outer diameter of the bearing, $D_4 = 0.05$ m.
2. $g = 0.001$ m and $g/D_4 = 0.02$.
3. For $g/D_4 = 0.02$, the optimum values of the design varaiables for selected configuration for the maximum bearing characteristics are presented in Table 4.

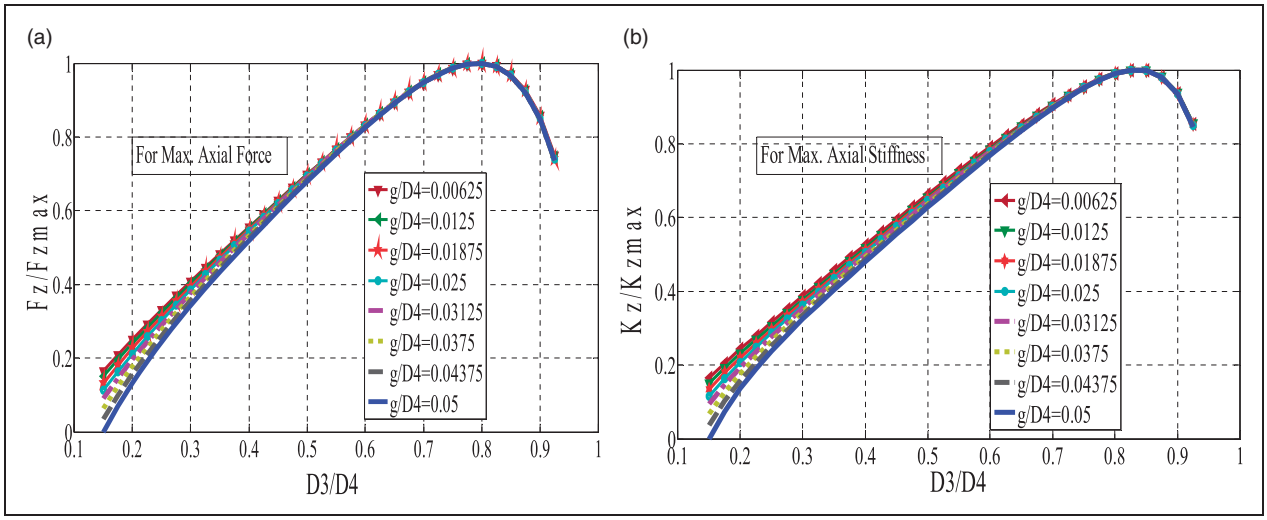

Figure 11. Optimized inner diameter of outer rings values as a function of air gap for maximized values of: (a) axial force and (b) stiffness.

Table 4. The optimum values of the design variables.

RMD configuration thrust bearing for maximum axial force	RMD configuration thrust bearing for maximum axial stiffness
Figure 8(a) $(h)_{opt}/D_4 = 0.0625 \rightarrow (h)_{opt} = 0.003125$ m, $\rightarrow$ i.e. $n = 12$	Figure 8(b) $(h)_{opt}/D_4 = 0.0375 \rightarrow (h)_{opt} = 0.001875$ m $\rightarrow$ i.e. $n = 20$
Figure 9(a) $(D_1)_{opt}/D_4 = 0.3 \rightarrow (D_1)_{opt} = 0.015$ m	Figure 9(b) $(D_1)_{opt}/D_4 = 0.45 \rightarrow (D_1)_{opt} = 0.0225$ m
Figure 10(a) $(D_3)_{opt}/D_4 = 0.8 \rightarrow (D_3)_{opt} = 0.04$ m	Figure 10(b) $(D_3)_{opt}/D_4 = 0.825 \rightarrow (D_3)_{opt} = 0.04125$ m

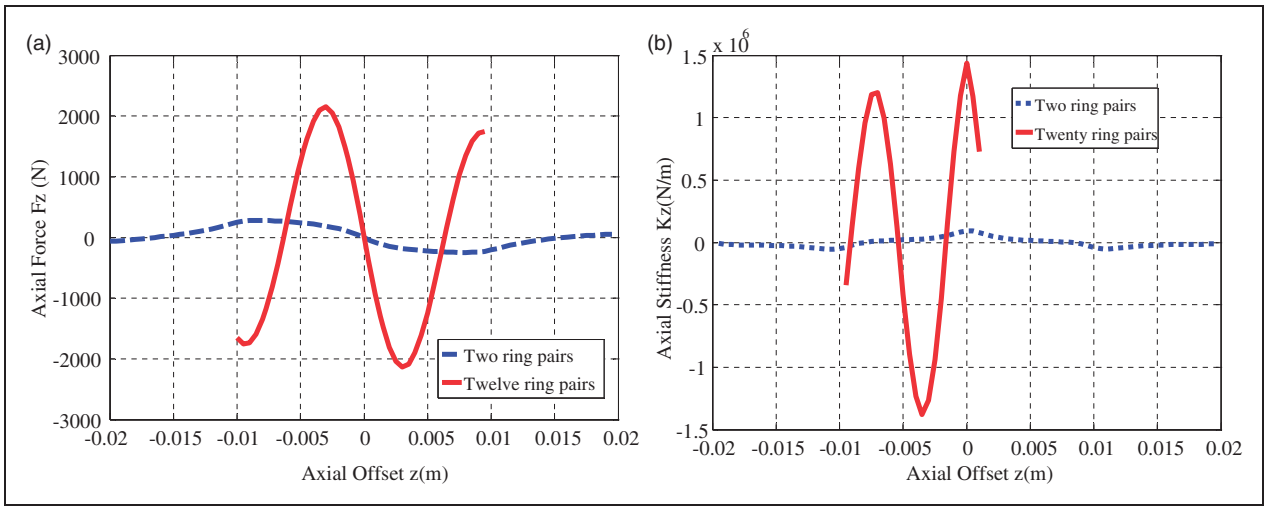

Figure 12. Optimized PM thrust bearing configuration results for: (a) axial force vs. axial offset and (b) axial stiffness vs. axial offset.

4. The maximized values of bearing characteristics in the optimized PM thrust bearing along with the results of two ring pairs in the selected control volume are presented in Figure 12. Results show that the axial force and stiffness generated in the optimized configuration is 7.6 (2151.86 N) and 15.34 (1,436,864.08 N/m) times the two ring pairs configuration results, respectively.

Comparison of the optimized results

Comparison of the results of the RMD configuration with the results of the conventional one as presented in Bekinal et al.,[21] optimized in the control volume with an aspect ratio of 0.5 is presented herewith. The results of comparison are provided in Table 5. It is observed that the maximized values of the axial force and stiffness in the RMD configuration are 1.98

Table 5. Comparison of the results of PM thrust bearing configurations with $B_r = 1.2$ T.

	RMD configuration		Conventional configuration[21]	
Optimized parameters	Optimized values for maximum axial force	Optimized values for maximum axial stiffness	Optimized values for maximum axial force	Optimized values for maximum axial stiffness
z (m)	0.0025	0	0.0025	0
n	8	12	4	6
R_1 (m)	0.006	0.009	0.004	0.0085
R_2 (m)	0.015	0.0155	0.015	0.0155
R_3 (m)	0.016	0.0165	0.016	0.0165
R_4 (m)	0.02	0.02	0.02	0.02
Maximized values	771.49 N	588,737.2 N/m	389.38 N	311,214.1 N/m
Volume of magnet (mm^3)	20,920	18,030	22,170	18,580

RMD: rotational magnetized direction.

(771.49 N) and 1.89 (588737.2 N/m) times that of the conventional one, respectively. The optimum number of rings at which force and stiffness are maximum in RMD is twice as compared to the conventional configuration. The volumes of magnet required to generate maximized force and stiffness in RMD are 0.94 (20,920 mm^3) and 0.97 (18,030 mm^3) times that of the conventional configuration in the control volume for an aspect ratio of 0.5.

Conlusions

MATLAB codes are developed to solve the generalized 3D equations of the axial force in RMD thrust bearing configuraion made up of n number of ring pairs for optimization in a given cylindical volume. Axial force values of the optimized configuration computed using proposed 3D equations are validated with the FEA results. The use of generalized plots for the optimization are very handy and useful as compared to 3D equations in optimizing the PM thrust bearing of any geometry. Such an approach shall pave away useful guidelines for industrial practices in adopting the proposed methodology with much ease.

Acknowledgements

The authors acknowledge the support of Sanjeevan Engineering and Technology Institute, Panhala and NITK, Surathkal for carrying out the research work.

Declaration of Conflicting Interests

The author(s) declared no potential conflicts of interest with respect to the research, authorship, and/or publication of this article.

Funding

The author(s) received no financial support for the research, authorship, and/or publication of this article.

ORCID iD

Siddappa Iranna Bekinal http://orcid.org/0000-0002-2942-2413

References

1. Jungmayr G, Marth E, Panholzer M, et al. Design of a highly reliable fan with magnetic bearings. *Proc IMechE, Part I: J Systems and Control Engineering* 2016; 230: 361–369.
2. Ohji T, Ichiyama S, Amei K, et al. Conveyance test by oscillation and rotation to a permanent magnet repulsive-type conveyor. *IEEE Trans Magn* 2004; 40: 3057–3059.
3. Kriswanto and Jamari. Radial forces analysis and rotational speed test of radial permanent magnetic bearing for horizontal wind turbine applications. In: *3rd international conference on advanced materials and science and technology (ICAMST 2015)*, *AIP conference proceedings*, Semarang, Indonesia, 2015, pp.020034-1-020034-10.
4. Fang J, Wang C and Tang J. Modeling and analysis of a novel conical magnetic bearing for vernier-gimballing magnetically suspended flywheel. *Proc IMechE, Part C: J Mechanical Engineering Science* 2014; 228: 2416–2425.
5. Bekinal SI, Jana S and Kulkarni SS. A hybrid (permanent magnet and foil) bearing set for complete passive levitation of high-speed rotors. *Proc IMechE, Part C: J Mechanical Engineering Science* 2017; 231: 3679–3689.
6. Sotelo GG, Andrade R and Ferreira AC. Magnetic bearing sets for a flywheel system. *IEEE Trans Appl Supercond* 2007; 17: 2150–2153.
7. Fang J, Le Y, Sun J, et al. Analysis and design of passive magnetic bearing and damping system for high-speed compressor. *IEEE Trans Magn* 2012; 48: 2528–2537.
8. Morales W, Fusaro R and Kascak A. Permanent magnetic bearing for spacecraft applications. *Tribol Trans* 2003; 46: 460–464.
9. Yonnet JP. Passive magnetic bearings with permanent magnets. *IEEE Trans Magn* 1978; 14: 803–805.

10. Yonnet JP. Permanent magnetic bearings and couplings. *IEEE Trans Magn* 1981; 17: 1169–1173.
11. Delamare J, Rulliere E and Yonnet JP. Classification and synthesis of permanent magnet bearing configurations. *IEEE Trans Magn* 1995; 31: 4190–4192.
12. Marth E, Jungmayr G and Amrhein W. A 2-D-based analytical method for calculating permanent magnetic ring bearings with arbitrary magnetization and its application to optimal bearing design. *Trans Magn* 2014; 50: 1–8.
13. Jiang S, Liang Y and Wang H. A simplified method of calculating axial force for a permanent magnetic bearing. *Proc IMechE, Part C: J Mechanical Engineering Science* 2010; 224: 703–708.
14. Ravaud R, Lemarquand G and Lemarquand V. Force and stiffness of passive magnetic bearings using permanent magnets. Part 1: Axial magnetization. *IEEE Trans Magn* 2009; 45: 2996–3002.
15. Ravaud R, Lemarquand G and Lemarquand V. Force and stiffness of passive magnetic bearings using permanent magnets. Part 2: Radial magnetization. *IEEE Trans Magn* 2009; 45: 3334–3342.
16. Samanta P and Hirani H. Magnetic bearing configurations: Theoretical and experimental studies. *IEEE Trans Magn* 2008; 44: 292–300.
17. Ravaud R, Lemarquand G and Lemarquand V. Halbach structures for permanent magnets bearings. *Prog Electromagn Res M* 2010; 14: 263–277.
18. Bekinal SI and Jana S. Generalized 3D Mathematical models for force and stiffness in axially, radially and perpendicularly polarized passive magnetic bearings with '*n*' number of ring pairs. *ASME J Tribol* 2016; 138: 31105(1–9).
19. Lijesh KP and Hirani H. Development of analytical equations for design and optimization of axially polarized radial passive magnetic bearing. *ASME J Tribol* 2015; 137: 1–9.
20. Moser R, Sandtner J and Bleuler H. Optimization of repulsive passive magnetic bearings. *IEEE Trans Magn* 2006; 42: 2038–2042.
21. Bekinal SI, Doddamani MR and Jana S. Optimization of axially magnetized stack structured permanent magnet thrust bearing using three-dimensional mathematical model. *ASME J Tribol* 2017; 139: 031101(1–9).
22. Xu FP, Li TC and Liu YJ. A study on passive magnetic bearing with Halbach magnetized array. In: *International conference on electrical machines and systems* (*ICEMS 2008*), Wuhan, China, 17–20 October 2008, pp.417–420.
23. Marth E, Jungmayr G, Panholzer M, et al. Optimization of stiffness per magnet volume ratio of discrete and continuous Halbach type permanent magnetic bearings. In: *13th international symposium on magnetic bearings (ISMB13)*, Arlington, Virginia, USA, 2012, pp.1–14.
24. Yoo SY, Kim WY, Kim SJ, et al. Optimal design of non-contact thrust bearing using permanent magnet rings. *Int J Precis Eng Manuf* 2011; 12: 1009–1014.
25. Safaeian R and Heydari H. Comprehensive comparison of different structures of passive permanent magnet bearings. *IET Electric Power Appl* 2017; 12: 179–187.
26. Bekinal SI, Doddamani MR and Dravid ND. Utilization of low computational cost two dimensional analytical equations in optimization of multi rings permanent magnet thrust bearings. *Prog Electromagn Res M* 2017; 62: 51–63.
27. Van Beneden M, Kluyskens V and Dehez B. Optimal sizing and comparison of permanent magnet thrust bearings. *IEEE Trans Magn* 2017; 53: 1–10.
28. Lijesh KP, Doddamani MR and Bekinal SI. A pragmatic optimization of axial stack-radial passive magnetic bearings. *ASME J Tribol* 2018; 140: 021901(1–9).